

Contract No.:

This manuscript has been authored by Savannah River Nuclear Solutions (SRNS), LLC under Contract No. DE-AC09-08SR22470 with the U.S. Department of Energy (DOE) Office of Environmental Management (EM).

Disclaimer:

The United States Government retains and the publisher, by accepting this article for publication, acknowledges that the United States Government retains a non-exclusive, paid-up, irrevocable, worldwide license to publish or reproduce the published form of this work, or allow others to do so, for United States Government purposes.

Photoconductive and electro-optic effects in (Cd,Mg)Te single crystals measured in an experiment-on-chip configuration

John Serafini,¹ A. Hossain,² R. B. James,^{2,3} M. Guziewicz,⁴ R. Kruszka,⁴ W. Słysz,⁴ and Roman Sobolewski^{1,5}

¹Department of Physics and Astronomy and Laboratory for Laser Energetics
University of Rochester, Rochester, NY 14627-0231, USA

²Brookhaven National Laboratory, Upton, NY 11973-5000, USA

³Savannah River National Laboratory, Aiken, NY 29803, USA

⁴Institute of Electron Technology, Warszawa, PL-02668 Poland

⁵Department of Electrical and Computer Engineering and Laboratory for Laser Energetics
University of Rochester, Rochester, NY 14627-0231, USA

Abstract

We present our studies on both photoconductive (PC) and electro-optic (EO) responses of (Cd,Mg)Te single crystals. In an In-doped Cd_{0.92}Mg_{0.08}Te single crystal, subpicosecond electrical pulses were optically generated via a PC effect, coupled into a transmission line, and, subsequently, detected using an internal EO sampling scheme. For both photo-excitation and EO sampling, we used femtosecond optical pulses generated by the same Ti:sapphire laser. The shortest transmission line distance between the optical excitation and EO sampling points was 75 μm . By measuring the transient waveforms at different distances from the excitation point, we calculated the transmission-line complex propagation factor and then reconstructed the electromagnetic transient generated directly at the excitation point, showing that the original PC transient was subpicosecond in duration with a fall time of ~ 500 fs. Finally, the measured EO retardation, together with the amount of the electric-field attenuation, allowed us to determine the magnitude of the internal EO effect in our (Cd,Mg)Te crystal. The obtained THz-frequency EO coefficient r_{41} was equal to 0.4 pm/V, which is at the lower end among the different values reported for CdTe-based ternaries, possibly due to the twinned structure of the tested (Cd,Mg)Te crystal.

Cadmium telluride is a very well studied II-VI semiconducting compound possessing a wide range of applications including solar cells [1, 2, 3], x-ray and gamma detectors [4] and optical modulators [5]. In addition, the incorporation of elements such as Zn, Mn, or Mg into the CdTe lattice results in tunable ternary compounds, that have led to a myriad of novel devices ranging from photoconducting and optoelectronic to magneto-optic. (Cd,Zn)Te is one of the main materials used as an x-ray and gamma-ray detector and is commercially available [6, 7], while (Cd,Mn)Te is among the best-known diluted magnetic semiconductors [8, 1]. In addition, (Cd,Mn)Te has been known for its interesting properties, both magneto- and electro-optic [9, 10], and recently has been successfully implemented in time-resolved x-ray detectors [11].

Cadmium magnesium telluride [(Cd,Mg)Te, (CMgT)] is the most-recent extension of the CdTe-based ternary family [12], but the extent of research performed on this material has been limited to its bulk properties [13, 14, 15, 16] consisting mainly of absorption and refractive nonlinearity studies [17]. As the other members of the family, Cd_{1-x}Mg_xTe has a stable zinc-blende crystalline structure and direct energy bandgap that can be linearly tuned for Mg concentrations x up to 0.70, while maintaining the parent lattice structure. In the case of the CMgT, however, this tuning range of the energy bandgap is the steepest, extending from the near infrared to the visible part of the spectrum [18]. The latter means that the optimal energy bandgap is attainable using the lower (as compared to other ternaries) content of Mg in CdTe and in this way minimizing lattice distortions and other alloy broadening effects. Another important advantage of CMgT is that its lattice constant is very similar to both MgTe and CdTe crystals, ensuring growth of high-quality CMgT single crystals with reduced stress. The latter features make CMgT a highly promising material for x and γ -ray detection, e.g., as a handheld radioisotope identifiers [12].

As the other members of the CdTe-based ternaries, CMgT has a non-centrosymmetric crystalline configuration, which permits the Pockels effect, i.e., a linear birefringence that can be induced on an appropriately polarized optical input beam [19, 20]. This type of electro-optic modulation is based on voltage-dependent retardance. For a polarized optical beam passing through a CMgT crystal, the phase retardation δ related to the Pockels effect is expressed as

$$\delta = \frac{2\pi n(\lambda)^3 r_{41} V L}{\lambda d}, \quad (1)$$

where $n(\lambda)$ is the refractive index of CMgT at a given wavelength λ of an optical input beam, V is the applied voltage, d is the electrode separation distance, r_{41} is the electro-optic coefficient, and L is the interaction length, i.e., penetration of the electric field through the crystal. The crystal only has one electro-optic term, r_{41} , because it is a member of the $\bar{4}3m$ -group point symmetry [19]. The phase retardation presented in Eq. (1) corresponds to the best-case scenario (the maximal EO effect), i.e., when the electric field vector E is aligned along the $\langle 110 \rangle$ crystalline direction, while the transmission line is deposited on the (110) surface of the CMgT crystal.

The aim of this paper is to demonstrate that highly resistive CMgT single crystals simultaneously exhibit strong photoconductive (PC) and electro-optic (EO) effects. In order to demonstrate this, we designed a so-called “experiment-on-chip” measurement, using a single, (110) oriented CMgT platelet with a deposited Au coplanar transmission line. Next, we optically triggered a sub-picosecond electrical transient using an ultraviolet pump pulse (surface excitation of carriers between a dc-biased coplanar transmission line), coupled it into the transmission line and, subsequently, time-resolved it with a subpicosecond resolution at a distance of $\sim 75 \mu\text{m}$ away from the excitation point with the help of an internal EO effect in the CMgT volume. An infrared probe pulse transmitted through a volume of the crystal was used in the measurement. The above arrangement allowed us to directly measure the CMgT photoconductive response and a subsequent nonequilibrium, intrinsic carrier relaxation dynamics in the CMgT crystal—these features are most important properties for the crystal radiation detection applications. At the same time, we managed to determine the magnitude of the EO effect in our CMgT material.

Our CMgT test samples were In-doped $\text{Cd}_{0.92}\text{Mg}_{0.08}\text{Te}$ single crystals grown using a vertical Bridgman method, following the procedure described in Ref. [12]. After the growth, the crystals were cut into (110)-oriented platelets and annealed in Cd vapor in order to improve their crystallinity and reduce the number of Cd vacancies, common for all Cd-based crystals. Subsequently, the surfaces were mechanically polished to remove any micro-scratches, followed by a chemical polishing in a 1% bromine-in-methanol solution. X-ray diffraction studies revealed that in our specimens the top surface, actually, deviated up to 10 degrees from the normal [110] direction. In addition, the crystals were strongly twinned and a twin mosaic had grains with sizes up about $20 \mu\text{m}$. The latter, as we show below, affected our ability to observe the maximal EO retardation, as described in Eq. (1). In the next step, the platelets were moved into a sputtering deposition system where they were pre-cleaned in an argon ion plasma at 300 V bias for 20 s in order to remove native oxides. A 200-nm-thick Au film was sputtered on the surface of the CMgT sample with a coplanar strip (CPS) transmission line patterned in a lift-off process that is shown in the bottom-right inset in Fig. 1. The CPS lines are $100\text{-}\mu\text{m}$ wide with a $25\text{-}\mu\text{m}$ gap.

Electrical characterization of our sample was carried out by measuring the dc current voltage (I-V) characteristics, both in the dark and under 400-nm pulsed light illumination with a nominal average power of 12 mW. The I-V curves (not shown) exhibited, in both cases, an ohmic behavior, and the resistivity of our crystals measured in the dark was on the level of $10^4 \Omega\text{-cm}$. The responsivity, calculated for a 12-mW light power with a $50\text{-}\mu\text{m}$ -diam spot size, linearly increased with the bias and reached a value of 22 mA/W at a 10-V bias, corresponding to a photon detection efficiency of $\sim 3.4\%$.

Time-resolved measurements of the CMgT photoresponse were performed using the laser system described in detail in [21]. Briefly, we used a mode-locked Ti:sapphire laser emitting a train of $\sim 100\text{-fs}$ pulses at 820-nm wavelength and a 76-MHz repetition rate. The laser output was split into two beams, designated as “the excitation and sampling trains,” respectively, using a 60/40

beam splitter. The train of excitation pulses was frequency doubled using a BaB₂O₄ crystal and modulated with an acousto-optic modulator operating at 243 kHz, while the sampling train, directly generated by the laser, was delayed with respect to the excitation pulse by passing through a computer-controlled delay stage. The excitation pulses were focused to a $\sim 50\text{-}\mu\text{m}$ -diameter spot to uniformly illuminate the gap between the dc-biased CPS lines, forming a so-called sliding contact [22] (see the bottom-right inset in Fig. 1) and triggering photo-generated electrical transients, which were launched into the CPS line. The sampling pulses, in turn, passed through a half-wave plate to align the beam polarization parallel to the electric-field transient generated across the transmission line via the PC effect. These pulses were focused to a $25\text{-}\mu\text{m}$ -diameter spot, and, finally, passed through the gap between the CPS lines. In the presence of an electric field from a propagating electrical transient, their polarization plane was tilted by δ degrees due to the Pockels (EO) effect, following Eq. (1). On the other side of the sample, the sampling beam was sent through a quarter-wave retarder that acted as a compensator, fed into a polarizing beam splitter, and, finally, detected by a pair of balanced photodetectors. The output from the photodetector was linked to a lock-in amplifier, which was synchronized to the modulation frequency of the pump beam. The 820-nm wavelength of the sampling train beam was chosen in order to assure that 1.52-eV energy of the sampling photons was not only below the 1.63-eV Cd_{0.92}Mg_{0.08}Te energy gap¹ but also below the band-tail states, which, in turn, would ensure high transmissivity of the sampling train through our 1-mm-thick CMgT platelet. Photoconductivity measurements with our sampling beam showed no significant response dismissing the possibility of excitation by two-photon absorption or ionization of deep levels. The system response was calibrated by measuring the voltage response (amount of birefringence) induced by a continuous-wave signal with an amplitude of 1.16 V and frequency of 243 kHz applied between the coplanar strip lines. The low-frequency EO sampler calibration has been done under a standard assumption that the EO effect is not sensitive to the electric field frequency as long as the energy of probing photons is below the energy gap of an EO crystal [23].

We collected a number of CMgT photoresponse transients at several distances away from the excitation point, ranging from $75\ \mu\text{m}$ to $325\ \mu\text{m}$. The transient recorded at the shortest distance, namely $75\ \mu\text{m}$, is presented in Fig. 1. The signal exhibits a 2.3-ps rise time (based on the 10% to 90% amplitude criterion), while its trailing edge represents the photo-carrier relaxation dynamics and can be very well fitted by a single exponential function with a decay time equal to 3.7 ps. Obviously, the temporal shape of the pulse is affected by a relatively long propagation distance from the excitation spot, which is discussed in the next paragraph. The top-right inset in Fig. 1 presents the same pulse, but it is shown on a much-longer time scale. We note that the main transient is followed by a series of post-pulses corresponding to the reflections from the contact pads located at both ends of the transmission line. The indicated $\sim 40\text{-ps}$ delay between the main

¹The energy gap was determined using a Perkin-Elmer Lambda 900 spectrometer; the value agrees well with the literature [12].

pulse and the first reflection peak corresponds to the round-trip distance between our sampling spot and the CPS biasing contacts, and the second feature is “a reflection of the reflection.”

Figure 2 shows the full-width-at-half-maximum (FWHM) values (solid circles) of the measured photoresponse as a function of the distance along the CPS line from the excitation spot. We note that the dependence is linear, as one would expect from the electric transient propagation in the quasi TEM regime. To determine the amount of distortion introduced by our CPS line, we performed a standard frequency-domain analysis of our signals [24] following an approach presented in [25]. First, we computed the frequency dependence of the complex propagation factor $\gamma(f)$ for our transmission line by dividing the frequency spectra of the waveforms measured at points 125 μm and 175 μm from the excitation spot. Next, knowing $\gamma(f)$, we numerically back-propagated one of the experimental transients toward its zero-distance plane (excitation spot) on the CPS line. The actual intrinsic transient generated by the photodetector is shown in the bottom-right inset in Fig. 2. We see that it has a peak amplitude of 730 mV, a FWHM of 600 fs, and a fall time of ~ 500 fs. The FWHM of the zero-distance pulse is indicated by the open circle in Fig. 2. Note that our intrinsic photoresponse signal has a 3-dB bandwidth up to 480 GHz and a 10% bandwidth above 1.8 THz. The signal’s leading edge corresponds to the integral of the excitation pulse (optical energy delivered), while the subpicosecond fall time indicates that our CMgT crystal must have a large number of shallow traps, and that trapping is the main relaxation mechanism [26]. The top-left inset in Fig. 2 presents the peak amplitudes (solid circles) of our experimentally measured photoresponse transients as a function of the propagation distance from the excitation point. As expected, the experimental data can be very well fitted (solid line) with an exponential decay and an attenuation constant of $\alpha = 0.005 \mu\text{m}^{-1}$.

In our experimental configuration, the CMgT crystal acts as an EO intensity modulator and measures the change in probe intensity that, subsequently, is recorded by the photodetector and read out by the lock-in as the voltage ΔV . Therefore, the differential transfer function of our EO sampling system is [27]

$$\frac{\Delta V}{V_0} = \frac{1}{2} \sin(\delta) \approx \frac{\delta}{2} \quad (2)$$

where V_0 is the dc component induced by our sampling beam with no excitation, and δ is given by Eq. (1). Throughout our measurements the $\Delta V/V_0$ ratio remained below 10^{-3} , so δ was always much smaller than π .

Figure 3 presents the measured ΔV values of our photoresponse transients as a function of the average power of the excitation train for a sampling train characterized by 100 μW of average power, a spot size diameter of 25 μm , and a CPS bias voltage of 10 V. We note that while for low pump powers, our data points follow a linear dependence, the overall dependence can be fitted very well (solid black line in the Fig. 3 main panel) using a saturable absorption-type curve $\sigma x/(1+\rho x)$ [28], where σ represents the linear response for small pump powers, and $1/\rho$ is the

power necessary to achieve a half the maximum response voltage. In our case, the linear response is $\sigma = 3 \mu\text{V}/\text{mW}$, while half the maximum response voltage occurs at 86 mW.

Next, by combining Eqs. (1) and (2), we calculated the EO coefficient r_{41} of our CMgT sample. As a reference point, we used the pump power of 12 mW, since most of our experiments were performed using this pump power (see, e.g., Figs. 1-2). Under these conditions, $\Delta V = 30 \mu\text{V}$ (Fig. 3) and the dc offset $V_0 = 0.15 \text{ V}$, corresponding to the static birefringence. Simultaneously, $n(\lambda=820 \text{ nm}) = 3.0$, determined by the independent ellipsometry measurements. The inset in Fig. 3 shows a simulated electric-field distribution across our 1-mm-thick CMgT crystal under CPS lines with the separation of $25 \mu\text{m}$ and applied transient peak voltage of 580 mV (see the main panel in Fig. 1). The bulk of the electric-field penetration is extended to about $200 \mu\text{m}$ under the crystal top surface. The latter value corresponds very well to the field penetration depth taken as the inverse of the attenuation α obtained from the top-left inset in Fig. 2, and was used in our calculations as the field interaction length L in Eq. (1). Using the above values, as well as the CMgT dielectric properties, i.e., its dielectric permittivity and the finite resistivity value, and the dimensions and parameters listed previously, we calculated r_{41} to be $\sim 0.4 \text{ pm}/\text{V}$. The latter value is near the lower end of the range of EO coefficients reported in literature for other CdTe-based ternaries [5]. It is possible, however, that our low value of r_{41} is to some extent due to the quality of the crystal we tested, i.e., a twin mosaic and the crystal surface 10° misorientation. Ultimately, see Eq. (1), one should use a twin-free crystal with a transmission line deposited on the (110) surface along the $\langle 100 \rangle$ crystalline direction, so the E field is along the $\langle 110 \rangle$ direction. Materials with a low concentration of tail-band states may also exhibit better EO properties.

In conclusion, we demonstrated simultaneous subpicosecond PC and EO effects, measured in the same CMgT single-crystal sample. The intrinsic PC transient, generated using 100-fs-wide, 410-nm-wavelength optical pulses, exhibited a 600-fs pulse width with an amplitude of over 700 mV. Only $75 \mu\text{m}$ away from the transient generation point, the signal was sampled in the same crystal via the internal EO effect with subpicosecond resolution. By sampling the PC transients at different points along the transmission line, we managed to fully characterize the propagation of the signal along the CPS line, specifically the attenuation constant, the inverse of which was used as the EO effect interaction length, allowing us to determine the THz-bandwidth EO coefficient, $r_{41} = 0.4 \text{ pm}/\text{V}$, for the In-doped $\text{Cd}_{0.92}\text{Mg}_{0.08}\text{Te}$ crystal. The observed subpicosecond photoresponse for CMgT demonstrates that these crystals should function well as ultrafast radiation detectors, and it is expected that ultrahigh-resistivity crystals ($>10^8 \Omega\text{-cm}$) would exhibit even better PC properties. Finally, CMgT also possesses an EO coupling coefficient in line with similar materials.

The authors would like to thank Christine Pratt and Stephen Burns for X-ray diffraction studies and Sudhir Trivedi and Dominika Kochanowska for fruitful discussions. This work was supported in part by the ARO Grant No. W911NF15-1-0356 and by the Pump Primer II Program at the University of Rochester. JS acknowledges support from the Frank Horton Graduate Fellowship Program at the University of Rochester's Laboratory for Laser Energetics, funded by

the U.S. Department of Energy. The support of ARO, University of Rochester, and DOE does not constitute their endorsement of the views expressed in this article.

References

- [1] J. K. Furdyna, "Diluted magnetic semiconductors," *Journal of Applied Physics*, vol. 64, p. R29, 1998.
- [2] B. E. McCannless and J. R. Sites, "Cadmium telluride solar cells," in *Handbook of Photovoltaic Science and Engineering*, England, John Wiley and Sons, 2003, pp. 617-662.
- [3] A. Rohatgi, R. Sudharasana, S. Ringel, P. Meyers, and C. Liu, "Growth and characterization of polycrystalline CdMnTe and CdZnTe thin films for solar cells," *Solar Cells*, vol. 24, pp. 185-194, 1988.
- [4] S. D. Sordo, L. Abbene, E. Caroli, A. M. Mancini, A. Zappettini, P. Ubertini, "Progress in the development of CdTe and CdZnTe semiconductor radiation detectors for astrophysical and medical applications," *Sensors*, vol. 9, pp. 3491-3526, 2009.
- [5] D. B. Chenault, R. A. Chapman, S-Y. Lu, "Electro-optic coefficient spectrum of cadmium telluride," *Applied Optics*, vol. 33, p. 7382, 1994.
- [6] R. B James, T. E. Schlesinger, P. Siffert and L. Franks, "Semiconductors for room temperature radiation detector applications," in *Materials Research Society Symposium Proceedings*, 1993.
- [7] M. Prokesch, S. A. Soldner, A. G. Sundaram, M. D. Reed, H. Li, J. F. Eger, J. L. Reiber, C. L. Shanor, C. L. Wray, A. J. Emerick, A. F. Peters, C. L. Jones, "CdZnTe detectors operating at X-ray fluxes of 100 million photons/(mm²-sec)," *IEEE Transactions on Nuclear Science*, vol. 63, p. 1854, 2016.
- [8] R. Rey-de-Castro, D. Wang, A. Verevkin, A. Mycielski, and R. Sobolewski, "Cd_{1-x}Mn_xTe Semimagnetic Semiconductors for Ultrafast Spintronics and Magneto Optics," *IEEE Trans. Nanotech*, vol. 4, pp. 106-112, 2005.
- [9] C.-C. Chen and J. F. Whitaker, "Combined nonlinear-optical electric and magnetic field response in a cadmium telluride crystal," *Applied Physics Letters*, vol. 92, p. 101119, 2008.
- [10] A. Mycielski, L. Kowalczyk, R. R. Galazka, R. Sobolewski, D. Wang, A. Burger, M. Sowinska, M. Groza, P. Siffert, A. Szadkowski, B. Witkowska, and W. Kaliszek, "Applications of II-VI semimagnetic semiconductors," *Journal of Alloys and Compounds*, vol. 423, pp. 163-168, 2006.
- [11] A. S. Cross, J. P. Knauer, A. Mycielski, D. Kochanowska, M. Witkowska-Baran, R. Jakięła, J. Domagała, Y. Cui, R. James, and R. Sobolewski, "(Cd,Mn)Te detectors for characterization of x-ray emissions generated during laser-driven fusion experiments," *Nuclear Instruments and Methods in Physics Research A*, vol. 624, pp. 649-655, 2010.
- [12] A. Hossain, V. Yakimovic, A. E. Bolotnikov, K. Bolton, G. S. Camarda, Y. Cui, J. Franc, R. Gul, K. H. Kim, H. Pittman, G. Yang, R. Herpst and R. B. James, "Development of cadmium magnesium telluride (Cd_{1-x}Mg_xTe) for room temperature x- and gamma-ray detectors," *Journal of Crystal Growth*, Vols.

250-267, p. 463, 2001.

- [13] S. Guha, J. E. Slagle, D. Lombardo and S. Trivedi, "Nonlinear optical properties of cadmium magnesium telluride," *Proceedings of SPIE*, vol. 9359, p. 93591, 2015.
- [14] K. Itoh, S. Nakashima, T. Fukumoto and A. Mitsuishi, "Lattice vibrations of CdMgTe-CdTe mixed crystals," *Journal of the Physical Society of Japan*, vol. 32, p. 1438, 1972.
- [15] K. Itoh and R. Yamamoto, "Preparation of electroluminescent properties of p-n junctions in $Cd_{(1-x)}Mg_xTe$," *Japanese Journal of Applied Physics*, vol. 8, p. 34, 1969.
- [16] Eunson Oh, C. Parks, I. Miotkowski, M. Dean Sciacca, A. J. Mayur, A. K. Ramdas, *Physical Review B*, vol. 48, p. 15040, 1993.
- [17] Guha, J. M. Murray, J. Wei, J. O. Barnes and J. E. Slagle and S., "Measuring refractive index using the focal displacement method," *Applied Optics*, vol. 53, pp. 3748-3752, 2014.
- [18] J. M. Hartmann, J. Cibert, F. Kany, H. Mariette, M. Charleux, P. Alloysson, R. Langer and G. Feuillet, "CdTe/MgTe heterostructures: Growth by atomic layer epitaxy and determination of MgTe parameters," *Journal of Applied Physics*, vol. 80, pp. 6257-6265, 1996.
- [19] A. Yariv, *Optical Electronics in Modern Communications*, New York: Oxford University Press, 1985.
- [20] K. Yang, T. Marshall, M. Forman, J. Jubert, L. Mirth, Z. Popovic, L. P. B. Katehi, and J. F. Whitaker, "Active-amplifier-array diagnostics using high resolution electro-optic field mapping," *IEEE Transactions on Microwave Theory Techniques*, vol. 49, pp. 849-857, 2001.
- [21] J. Serafini, Y. Akbas, L. Crandal, C. K. Williams, R. Bellman, and Roman Sobolewski, "Time-resolved, nonequilibrium carrier dynamics in Si-on-glass thin-film absorbers for photovoltaic cells," *Semiconductor Science and Technology*, vol. 31, p. 045006, 2016.
- [22] M. B. Ketchen, D. Grischkowsky, T. C. Chen, C. Chi, I. N. Duling, N. J. Halas, J.-M. Halbout, J. A. Kash, and G. P. Li, "Generation of subpicosecond electrical pulses on coplanar transmission lines," *Applied Physics Letters*, vol. 48, p. 751, 1986.
- [23] G. A. Mourou and K. E. Meyer, "Subpicosecond electro-optic sampling using coplanar strip transmission lines," *Applied Physics Letters*, vol. 45, pp. 492-494, 1984.
- [24] J. F. Whitaker, R. Sobolewski, D. R. Dykaar, T. Y. Hsiang, and G. A. Mourou, "Propagation model for ultrafast signals on superconducting dispersive striplines," *IEEE Transactions on Microwave Theory and Techniques*, vol. 36, pp. 277-285, 1988.
- [25] M. Mikulics, J. Zhang, J. Serafini, R. Adam, D. Grutzmacher and R. Sobolewski, "Subpicosecond

electron-hole recombination time and terahertz-bandwidth photoresponse in freestanding GaAs epitaxial mesoscopic structures," *Applied Physics Letters*, vol. 101, p. 031111, 2012.

- [26] J. Serafini, F. Song, R. Sobolewski, "Ultrafast characterization of CdMgTe single crystals," *In preparation*, 2016.
- [27] A. Cross, D. Kochanowska, M. Witkowska-Baran, A. Mycielski, M. Mikulics, D. Grutzmacher, R. Sobolewski, "Femtosecond electro-optic effect in (Cd,Mn)Te single crystals," *Journal of Physics: Conference Series*, vol. 194, p. 012057, 2009.
- [28] Y. Gao, X. Zhang, Y. Li, H. Liu, Y. Wang, Q. Chang, W. Jiao, and Y. Song., "Saturable absorption and reverse saturable absorption in platinum nanoparticles," *Optics Communications*, vol. 251, pp. 429-433, 2005.
- [29] S.D. Sordo, L. Abbene, E. Caroli, A. M. Mancini, A. Zappettini and P. Ubertini, "Progress in the Development of CdTe and CdZnTe," *Sensors*, vol. 9, pp. 3491-3526, 2009.
- [30] Y. Cui, A. Bolotnikov, G. Carmarda, A. Hossain, G. Yang, R. B. James, "CZT virtual Frisch-grid detector: Principles and applications," in *Proceedings 5th Annual IEEE Long Island Systems, Applications and Technology Conference*, Farmingdale, NY, 2009.

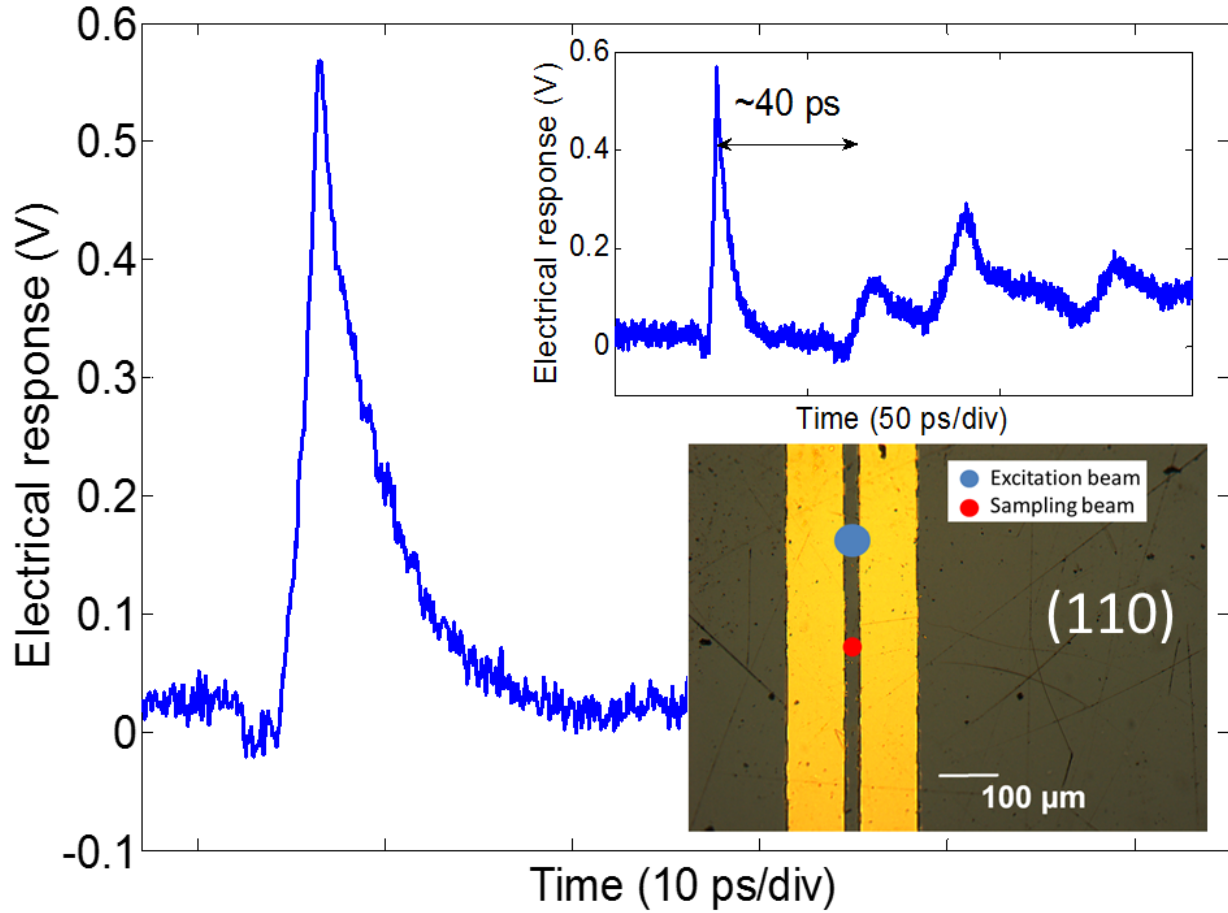


Figure 1: A time-resolved CMgT photoconductive response measured at $75 \mu\text{m}$ from the excitation spot via the electro-optic effect. The top-right inset shows the same signal but in a larger time window, showing the post-pulse peaks caused by the reflection of the optical pulse at the bias contacts, 2.5-mm away from the probe site. The bottom-right inset features a picture of our CPS lines fabricated on a (110) surface of the CMgT crystal with the excitation and sampling beams indicated, blue and red dots marks, respectively. The excitation average power was 12 mW, and the pump-pulse wavelength was 410 nm. The CPS line DC bias was 10 V.

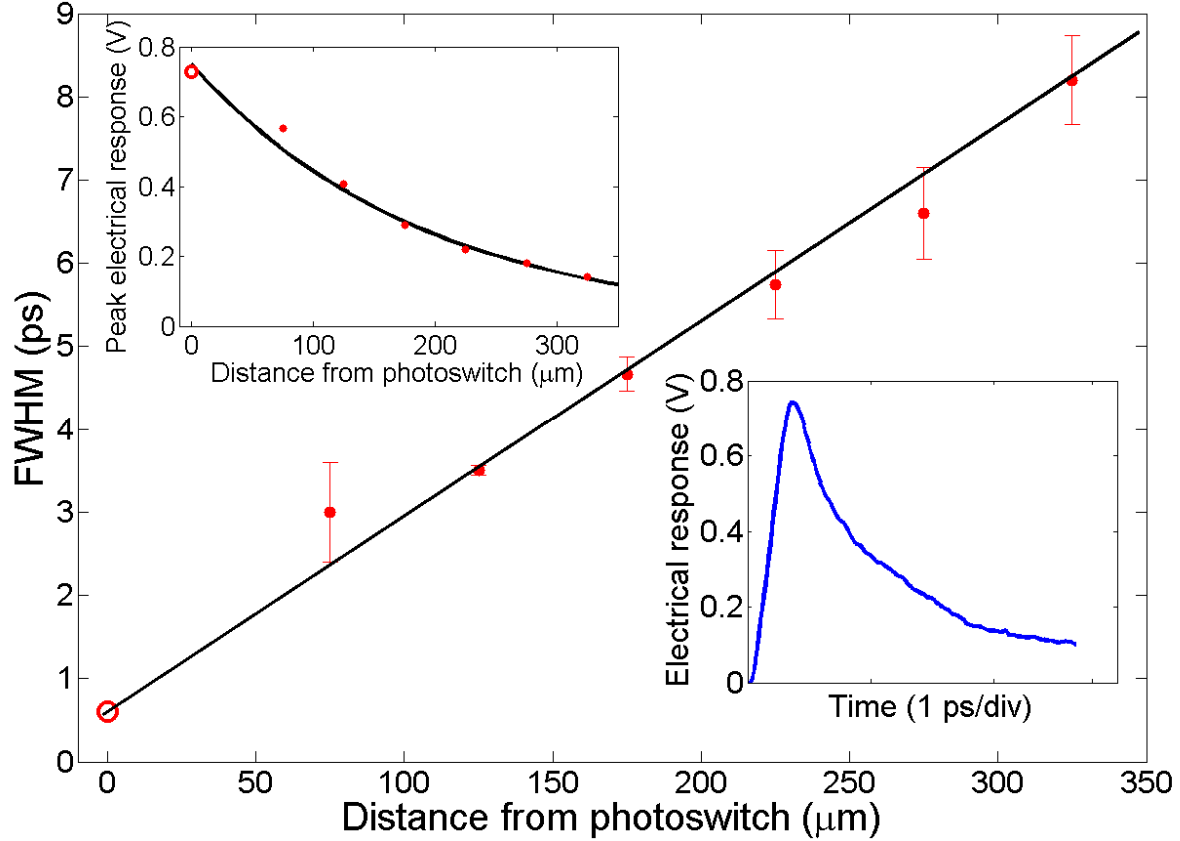


Figure 2: Full width at half maximum of the photoresponse pulses recorded at different distances from the photoswitch. All measurements (solid circles) were performed using the pump pulses with 12 mW of averaged power. The open circle denotes our intrinsic, “back-propagated” pulse. The sampling train had an averaged power of 1 mW and 820-nm wavelength. The 600-fs FWHM of the intrinsic pulse (open circle) was calculated using the methods of Whittaker et al. [24]. The simulated waveform of the intrinsic pulse (at zero propagation distance) is included in the bottom-right inset. The top-left inset shows the peak voltages of pulses sampled at different distances from the photoswitch (red dots) and the single-exponential fit (black line) with an attenuation constant $\alpha = 0.005 \mu\text{m}^{-1}$.

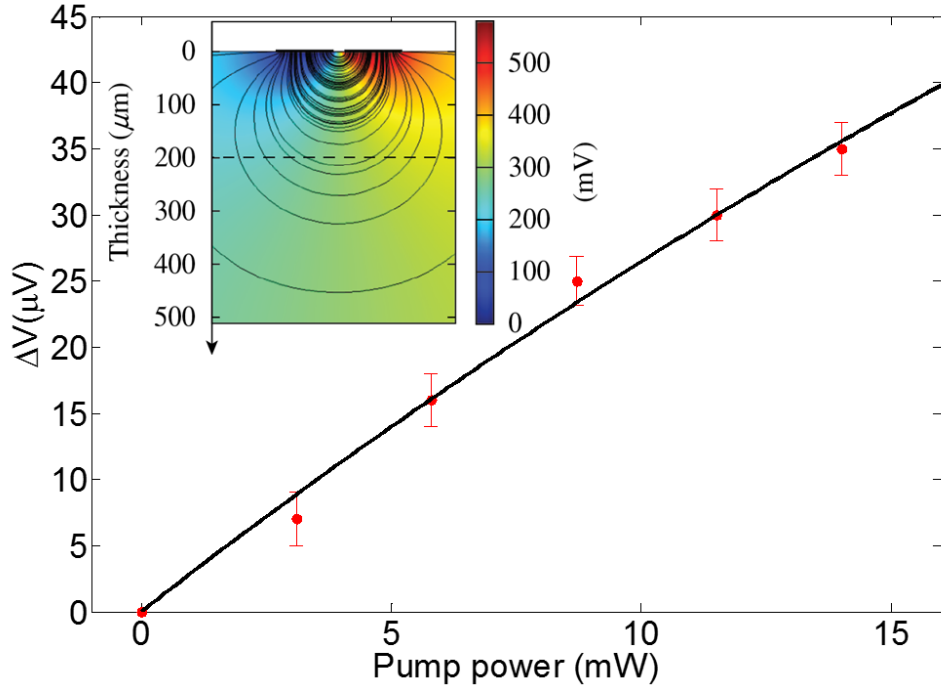


Figure 3: Amplitude of the PC-generated pulses (red dots) as a function of pump power with the sampling beam held fixed at $100 \mu\text{W}$ at 820 nm , and the bias fixed at 10 V . The data points were fit (black line) to a saturable absorption model having the initial linear response of $\sim 3 \mu\text{V}/\text{mW}$. The inset features a COMSOL simulation of the electric-field distribution throughout our 1-mm-thick CMgT crystal. The simulation assumes a 580-mV, transient-peak voltage amplitude across the CPS line, as measured at the distance of $75 \mu\text{m}$ from the excitation point (see Fig. 1).